Progress In Electromagnetics Research, Vol. 133, 159–176, 2013

UNIDIRECTIONAL ANTENNA USING TWO-PROBE EXCITED CIRCULAR RING ABOVE SQUARE REFLECTOR FOR POLARIZATION DIVERSITY WITH HIGH ISOLATION

S. Vongsack[1], C. Phongcharoenpanich[1, *], S. Kosulvit[1], K. Hamamoto[2], and T. Wakabayashi[3]

[1]Faculty of Engineering, King Mongkut's Institute of Technology Ladkrabang, Bangkok 10520, Thailand

[2]School of Information and Telecommunication Engineering, Tokai University, 1117 Kitakaname, Hiratsuka, Kanagawa 259-1292, Japan

[3]Malaysia-Japan International Institute of Technology, University of Technology Malaysia, Kuala Lumpur 54100, Malaysia

Abstract—This paper presents a circular ring antenna fed by two perpendicular probes, both of which are placed above the square reflector. The antenna is employed to radiate unidirectional beam for polarization diversity reception. A linear isolator is added to improve the isolation between the two probes. The antenna is proposed for the point-to-point communication of Wireless Local Area Network (WLAN) system according to the IEEE 802.11a standard in which the allocated frequency band ranges from 5.150 GHz to 5.825 GHz. The proposed antenna is compact and suitable for mass production. Without the dielectric material, the antenna is free of dielectric loss and capable of high power handling. The prototype antenna was fabricated and measured to verify the theoretical predictions. At the center frequency, the unidirectional pattern with the measured half-power beamwidths in two principal planes of 65 and 75 degrees is achieved. The front-to-back ratio is 31 dB, and the antenna gain is 7.42 dBi. The $|S_{11}|$ and $|S_{21}|$ are respectively -23.09 dB and -33.99 dB; the obtained bandwidth is 23.64%. Based on the aforementioned characteristics, the antenna is a potential candidate for polarization diversity of WLAN applications.

Received 1 August 2012, Accepted 15 October 2012, Scheduled 18 October 2012

* Corresponding author: Chuwong Phongcharoenpanich (pchuwong@gmail.com).

1. INTRODUCTION

Presently, wireless communications are essential for human activities in various aspects. The Wireless Local Area Network (WLAN) system plays an important role in connecting users in the community of a given service area [1]. Based on IEEE 802.11a standard, the operating frequency band covers 5.150 GHz to 5.825 GHz, of which the center frequency is 5.5 GHz [2]. Typically, the communication network of WLAN system can be classified into two topologies, i.e., point-to-multipoint and point-to-point connections. The point-to-multipoint connection is the typical topology in which the root or base station is able to communicate to a number of clients located around it. In this configuration, the omnidirectional antenna is suitable for the base station [3–9]. For the point-to-point connection topology, the unidirectional antenna is a promising candidate [10–12]. In the case of only line of sight (LOS) situation, the signal can be directly propagated from the transmitter to the receiver. However, in some environments in which the transmitter and receiver are obstructed by various objects, the multipath signal occurs due to obstacles, such as buildings and trees, which cause the signal to reflect and diffract. The multiple components of transmitted signal reach the receiver at slightly different time points, thereby producing multipath fading which not only varies with time and physical motion but also affects the channel performance and thus reduces the data rate [13]. To mitigate the fading problem, the diversity reception techniques have been applied [14, 15]. A number of diversity antennas have been discussed in the existing literature [16, 17]. The space diversity with proper spacing between two antennas is the simplest geometry [18]. However, since large spacing is required, the overall antenna dimension needs to be relatively large [19]. The polarization diversity with two orthogonal excitations in the same antenna body has been proposed to minimize the whole antenna size [20–23]. The polarization diversity antenna with unidirectional pattern is very useful for base station applications such as WLAN system [24–35]. This paper presents the unidirectional antenna for polarization diversity of WLAN system following IEEE 802.11a standard with the operating frequency band between 5.150 GHz and 5.825 GHz. The antenna evolution starts from the circular ring excited by a probe that radiates bidirectional pattern in two opposite directions along two ring apertures with single polarization. This structure is located above the square reflector to confine the main beam to single direction. The excitation with two perpendicular probes is introduced for polarization diversity. To improve the isolation between two excited probes, the linear isolator

with proper angle is added. The antenna characteristics in terms of the reflection ($|S_{11}|$ and $|S_{22}|$), isolation ($|S_{21}|$ and $|S_{12}|$), radiation pattern, and gain are presented. The simulation was performed using CST Microwave Studio [36]. The prototype antenna was fabricated and measured to confirm the theoretical principle.

The organization of this paper is as follows. The proposed antenna structure and its associated parameters are discussed in Section 2. Section 3 addresses the design principle and parametric study and in Section 4 the measured results are presented. The conclusions are drawn and detailed in Section 5.

2. ANTENNA STRUCTURE

The antenna configuration consists of a circular ring with radius r_a, length d and thickness t as shown in Fig. 1(a). The center of the ring is located at the origin of yz-plane. This ring is excited by two identical probes in the radial direction of the length l_f and radius r_f via 50-Ω SMA connector. The first probe (Probe1) is aligned on z-axis to generate vertical polarization whereas the other probe (Probe2) is oriented along y-axis to create horizontal polarization. The linear isolator of the length l_p and radius r_p is situated inside the ring in the radial direction between two probes. The position of the isolator is at an angle α relative to the Probe1. This structure is placed above the square reflector of size L. The spacing between the ring and the

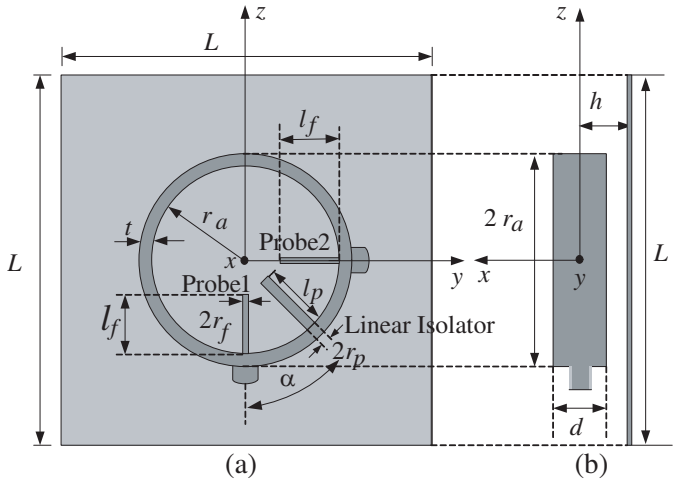

Figure 1. The proposed antenna structure. (a) Perspective view. (b) Side view.

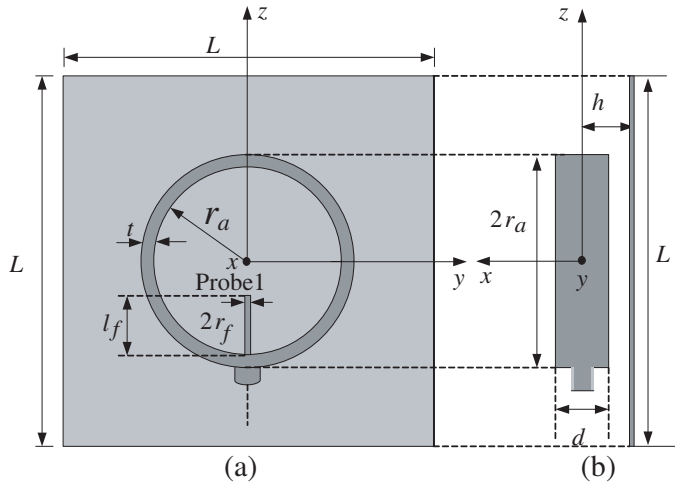

Figure 2. An initial antenna structure. (a) Perspective view. (b) Side view.

reflector is denoted with h as illustrated in Fig. 1(b). The radiation pattern of this antenna is unidirectional with the beam peak pointing x direction.

3. DESIGN PRINCIPLE AND PARAMETRIC STUDY

The antenna structure is designed to operate along the frequency range of 5.150 GHz to 5.825 GHz, of which the center frequency is 5.5 GHz. The principle of the antenna design starts with the conventional circular ring as shown in Fig. 2, with the initial radius $(r_a)\lambda/2$ of the center frequency, which is equal to 2.727 cm. The ring is excited by a single probe of the length $(l_f)\lambda/4$ or 1.363 cm. It is noted that the ring in this paper is made of aluminum with the thickness t of 3 mm. The ring length d of 1.527 cm (0.28λ) and probe radius r_f of 0.65 mm (0.011λ) are selected and used throughout the design due to its ubiquity as fabrication material. The ring length (d) affects to the directivity of the antenna. The guideline for the selection of d for the desired directivity can be found in [37]. To keep the antenna as compact as possible, the size of the square reflector is chosen to be 8 cm with the spacing between the circular ring and the square reflector h of 1.418 cm (0.26λ). In addition, the influence of the size of the square reflector and the spacing between the circular ring and the square reflector will be clarified in this section. It is noted that the infinitesimal gap between the circular ring and the linear isolator is separated with dielectric supporter. There is no electrical contact between the circular ring and the linear isolator.

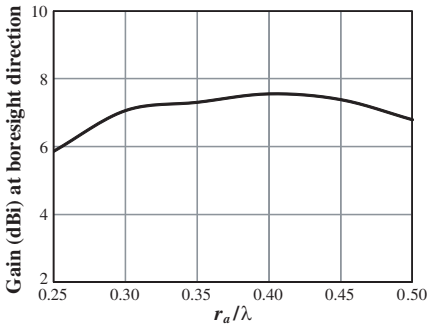

Figure 3. The gain at boresight direction versus ring radius r_a ($l_f = 1.36\,\text{cm}$ and $r_f = 0.65\,\text{mm}$).

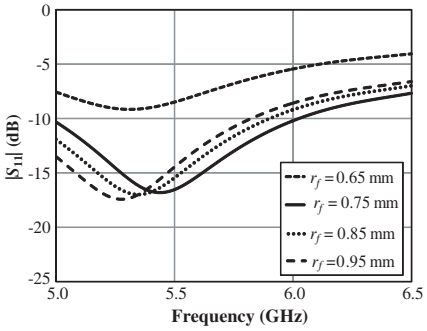

Figure 4. The $|S_{11}|$ versus frequency for various probe radii r_f ($r_a = 2.18\,\text{cm}$ and $l_f = 1.36\,\text{cm}$).

To determine the proper antenna dimensions that meet the optimum characteristics and are of compact size, the antenna parametric study will be carried out. Fig. 3 illustrates the gain at the boresight direction ($\theta = 90°$, $\phi = 0°$) of the circular ring antenna excited by the single probe above the square reflector for various ring radii r_a. It is evident that the radius of 0.4λ yields the maximum gain. Therefore, the ring radius r_a of 2.18 cm (0.4λ) is selected as the design parameter.

To obtain the good matching condition with efficiently wide bandwidth, the probe radius is adjusted in an incremental fashion of 0.1 mm. Fig. 4 shows the $|S_{11}|$ at single probe excitation versus frequency of the proposed antenna for various probe radii r_f. It is obvious that the probe radius affects the frequency of the minimum $|S_{11}|$. For $r_f = 0.65\,\text{mm}$, the $|S_{11}|$ is unacceptable due to the reflection level greater than $-10\,\text{dB}$ throughout the desired frequency band. When r_f is increased to 0.75 mm or higher, the level of the minimum $|S_{11}|$ at 5.5 GHz is less than $-15\,\text{dB}$. To achieve the minimum $|S_{11}|$ at the center frequency, r_f of 0.75 mm is selected. The bandwidth coverage is from 5 GHz to 6 GHz.

To develop the circular ring antenna above square reflector for polarization diversity reception, two perpendicular excitation probes in z direction (Probe1) and y direction (Probe2) are introduced as shown in Fig. 1. By adding Probe2 inside the ring, the reflection at each probe (in terms of $|S_{11}|$ and $|S_{22}|$) is degraded compared with when merely Probe1 excitation is employed. Fig. 5 illustrates the frequency response of the reflection of each probe (in terms of $|S_{ii}|$) and the isolation between two probes (in terms of $|S_{ij}|$). It is noted that $|S_{11}|$ and $|S_{22}|$ are identical because of their symmetrical structure while $|S_{21}|$ and

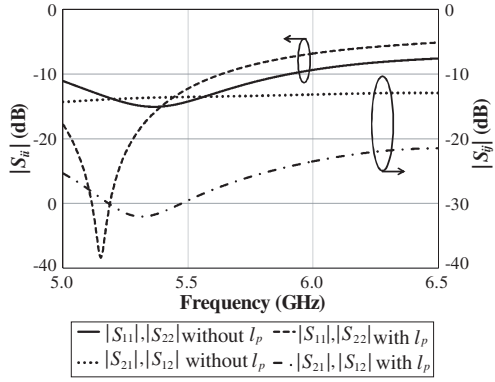

Figure 5. The reflection ($|S_{ii}|$) and the isolation ($|S_{ij}|$) versus frequency with and without linear isolator ($r_a = 2.18\,\text{cm}$, $l_f = 1.36\,\text{cm}$, $r_f = 0.75\,\text{mm}$, $l_p = 1.60\,\text{cm}$, $r_p = 2.50\,\text{mm}$, and $\alpha = 45°$).

$|S_{12}|$ are identical due to reciprocal property. The solid line indicates the $|S_{11}|$ and $|S_{22}|$ when two perpendicular probes are employed. It is noted that $|S_{11}|$ is taken into account when Probe1 is excited and while Probe2 is terminated with the matched load. Meanwhile, $|S_{22}|$ is the result of excitation at Probe2 whereas Probe1 is matched with the dummy load termination. As illustrated by the solid line in Fig. 5, $|S_{11}|$ worsens with merely one probe excitation due to the coupling effect from Probe2. In terms of $|S_{ij}|$ of the isolation (inverse of coupling) where $i \neq j$, it could be observed from the dotted line that $|S_{21}|$ is around $-14\,\text{dB}$ along the frequency band. The isolation in this case is relatively low and insufficient for practical applications. To improve the isolation, the simple linear isolator is symmetrically oriented between the two probes at an angle α of 45°. The linear isolator is made of the copper rod. It is a resonant component that is used to block the surface current from Probe1 to Probe2. Note that the infinitesimal gap between the circular ring and the linear isolator is separated with dielectric supporter to prevent the electrical connection. The current from Probe1 will be stored by this linear isolator. By considering the dashed line and dash-dotted line in Fig. 5, the $|S_{11}|$ and $|S_{21}|$ with the linear isolator included are remarkably improved. However, the $|S_{11}|$ and $|S_{21}|$ are not optimum at the center frequency.

The parametric study of the probe length l_f, isolator length l_p and angle α between the isolator and Probe1 will be the focus of this section. Fig. 6 shows the $|S_{11}|$ and $|S_{21}|$ along the frequency range of 5.0–6.5 GHz for different probe lengths l_f. The probe length influences both the frequency and the level of minimum $|S_{11}|$. To obtain the minimum $|S_{11}|$ at the center frequency of 5.5 GHz, l_f of 1.25 cm is

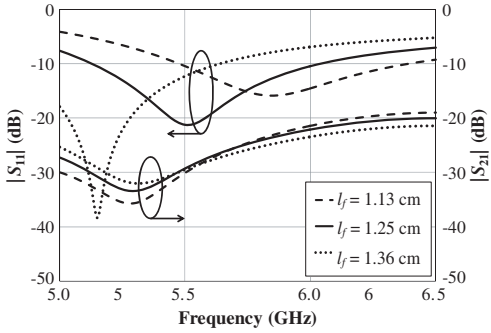

Figure 6. The $|S_{11}|$ and $|S_{21}|$ versus frequency for various probe lengths l_f ($r_a = 2.18\,\text{cm}$, $r_f = 0.75\,\text{mm}$, $l_p = 1.60\,\text{cm}$, $r_p = 2.50\,\text{mm}$ and $\alpha = 45°$).

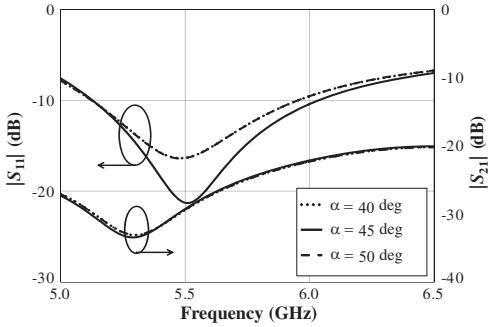

Figure 7. The $|S_{11}|$ and $|S_{21}|$ versus frequency for various angles α between the isolator and Probe1 ($r_a = 2.18\,\text{cm}$, $l_f = 1.25\,\text{cm}$, $r_f = 0.75\,\text{mm}$, $l_p = 1.60\,\text{cm}$ and $r_p = 2.50\,\text{mm}$).

explicitly chosen. However, when the probe length is varied, the level of $|S_{21}|$ only slightly changes. In particular, at the center frequency, $|S_{21}|$ of different probe lengths are almost identical. The level of $|S_{21}|$ is around $-30\,\text{dB}$; therefore, l_f of $1.25\,\text{cm}$ is the optimum length.

The angle α between the linear isolator and Probe1 is another parameter to be investigated. Fig. 7 shows the $|S_{11}|$ and $|S_{21}|$ versus frequency for various angles α. It is noted that the $|S_{11}|$ of angle α between the isolator and Probe1 and the $|S_{22}|$ of angle $90° - \alpha$ between the isolator and Probe2 are identical because Probe1 and Probe2 are perpendicular to each other. It is found that $|S_{11}|$ at α of 45° has the minimum $|S_{11}|$ of $-21.25\,\text{dB}$. When the isolator is located offset from the middle between two probes, $|S_{11}|$ becomes worse. The angle between the isolator and the probe has no influence upon the isolation. Therefore, $\alpha = 45°$ is chosen as the design parameter.

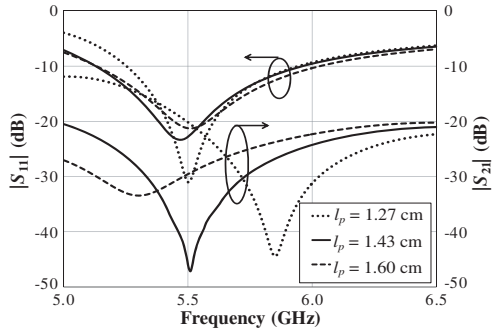

Figure 8. The $|S_{11}|$ and $|S_{21}|$ versus frequency for various isolator lengths l_p ($r_a = 2.18\,\text{cm}$, $l_f = 1.25\,\text{cm}$, $r_f = 0.75\,\text{mm}$, $r_p = 2.50\,\text{mm}$ and $\alpha = 45°$).

The isolator length l_p is subsequently varied to achieve the optimum reflection and isolation. Fig. 8 shows the $|S_{11}|$ and $|S_{21}|$ of the antenna for various isolator lengths. It is apparent that the isolator length has affected the level of minimum $|S_{11}|$. For $|S_{21}|$ characteristic, when the isolator length is increased, the frequency of minimum $|S_{21}|$ is lower. To achieve the minimum $|S_{21}|$ at 5.5 GHz, the isolator length l_p of 1.43 cm is selected. At the center frequency of 5.5 GHz, the obtained $|S_{11}|$ and $|S_{21}|$ are respectively $-22.79\,\text{dB}$ and $-46.54\,\text{dB}$. It is explicit that the added linear isolator can significantly improve the isolation between the two probes with good reflection at each probe.

The spacing between the circular ring and the square reflector (h) is another parameter that is necessary to be appropriately determined. Fig. 9 shows the $|S_{11}|$ and $|S_{21}|$ of the proposed antenna versus frequency for various spacing between the circular ring and the square reflector h. The reflection and isolation of the antenna are changed with the variation of h. To achieve the optimum $|S_{11}|$ and $|S_{21}|$, h of 1.41 cm is obviously chosen. When h is smaller, the $|S_{11}|$ is slightly lower, but the minimum $|S_{11}|$ is occurred at the higher frequency. The isolation of the smaller h is drastically lower. For h of larger than 1.41 cm, the reflection and isolation become worse.

The unidirectional beam is achieved by placing the circular ring above the square reflector. The square reflector size must be selected according to the compact size and good electrical characteristics. The $|S_{11}|$ and $|S_{21}|$ for various sizes of the square reflector is illustrated in Fig. 10. It is apparent that the reflection and isolation are not significantly sensitive with the size of the square reflector. To obtain the optimum $|S_{11}|$ and $|S_{21}|$, the square reflector size of 8 cm is chosen. Generally, the square reflector size has impacted on the radiation pattern especially the front-to-back (F/B) ratio. Fig. 11

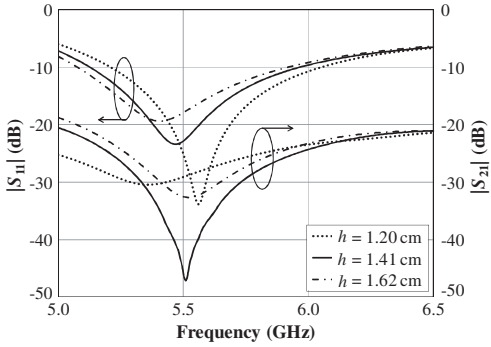

Figure 9. The $|S_{11}|$ and $|S_{21}|$ versus frequency for various spacing between probe and reflector h ($r_a = 2.18\,\text{cm}$, $l_f = 1.25\,\text{cm}$, $r_f = 0.75\,\text{mm}$, $r_p = 2.50\,\text{mm}$, $\alpha = 45^\circ$ and $l_p = 1.43\,\text{cm}$).

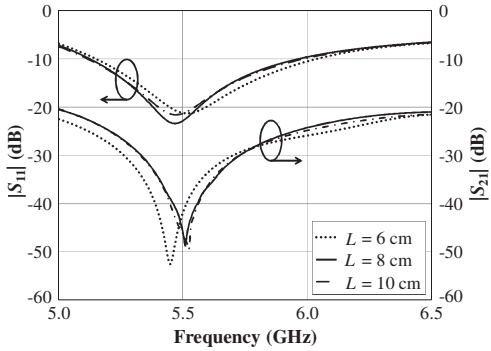

Figure 10. The $|S_{11}|$ and $|S_{21}|$ versus frequency for various square reflector size L ($r_a = 2.18\,\text{cm}$, $l_f = 1.25\,\text{cm}$, $r_f = 0.75\,\text{mm}$, $r_p = 2.50\,\text{mm}$, $\alpha = 45^\circ$ and $l_p = 1.43\,\text{cm}$).

shows the radiation pattern of the antenna in xy- and xz-plane for either Probe1 or Probe2 excitation. The unidirectional pattern with similar beamwidth is obtained with the square reflector size of 6 cm, 8 cm and 10 cm. As expected, the F/B ratio is lower when the square reflector size is smaller. To obtain the compact size with F/B ratio higher than 20 dB, the square reflector size L of 8 cm is accordingly chosen.

Based on the parametric study results, the design parameters of the proposed antenna are tabulated in Table 1.

The radiation pattern of the antenna in two principal planes for excitation of Probe1 and Probe2 is illustrated in Figs. 12(a)

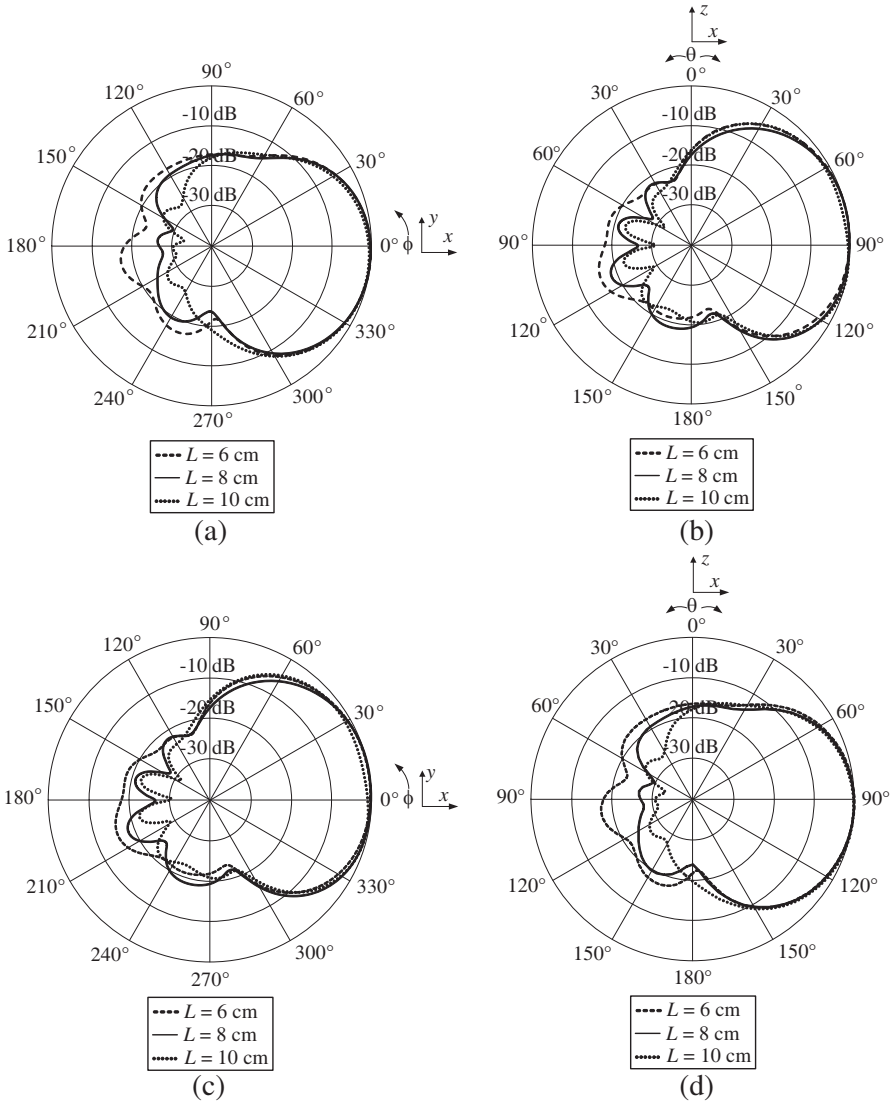

Figure 11. The radiation pattern at 5.5 GHz for various L (r_a = 2.18 cm, l_f = 1.25 cm, r_f = 0.75 mm, l_p = 1.43 cm, r_p = 2.50 mm and $\alpha = 45°$). (a) Probe1 excitation in xy plane. (b) Probe1 excitation in xz plane. (c) Probe2 excitation in xy plane. (d) Probe2 excitation in xz plane.

Table 1. The design parameters.

Parameter	Electrical size	Physical size line at 5.5 GHz
L	1.466λ	8.000 cm
r_a	0.400λ	2.181 cm
d	0.280λ	1.527 cm
t	0.055λ	3.000 mm
h	0.260λ	1.418 cm
l_f	0.229λ	1.250 cm
r_f	0.013λ	0.750 mm
l_p	0.262λ	1.430 cm
r_p	0.045λ	2.500 mm
α	45°	

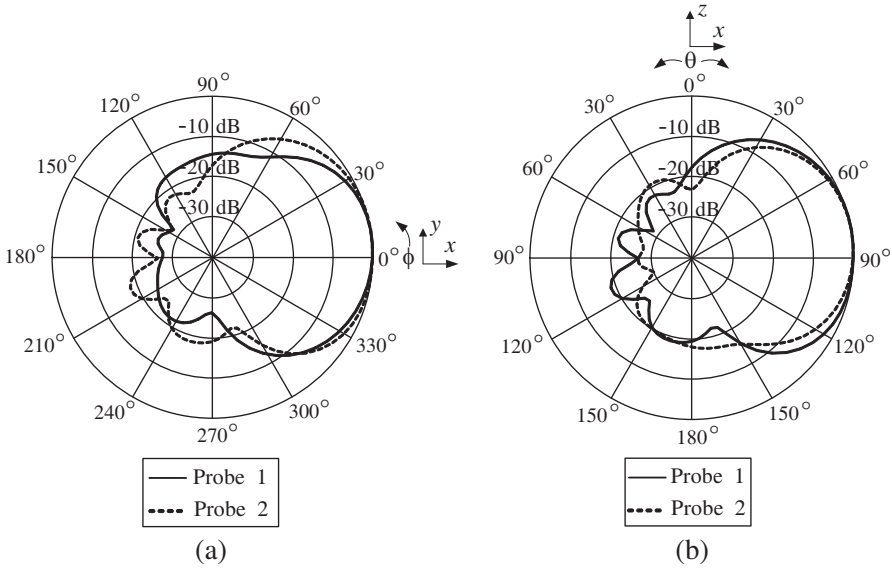

Figure 12. The radiation pattern at 5.5 GHz ($r_a = 2.18$ cm, $l_f = 1.25$ cm, $r_f = 0.75$ mm, $l_p = 1.43$ cm, $r_p = 2.50$ mm and $\alpha = 45°$). (a) xy plane. (b) xz plane.

and 12(b) in which the radiation patterns in xy-plane and xz-plane are respectively shown. The solid line represents the excitation of Probe1 whereas the dashed line is for Probe2 excitation. The unidirectional pattern is achieved for either Probe1 or Probe2 excitation. It is noted that the pattern in xy-plane for Probe1 excitation is identical to that in

xz-plane for Probe2 excitation due to the symmetrical configuration in two principal planes. The half-power beamwidths (HPBW) in xy-plane for excitation of Probe1 and Probe2 are 60 degrees and 80 degrees, respectively. The F/B ratio in both planes is 26 dB.

4. MEASURED RESULTS

To verify the antenna principle, the prototype antenna with the design parameters tabulated in Table 1 was fabricated as depicted in Fig. 13.

The reflection (in terms of $|S_{11}|$) and isolation (in terms of $|S_{21}|$) were measured using an HP872C Network Analyzer. It is noted that $|S_{11}|$ was measured at input port of Probe1 while Probe2 was terminated with matched load. Fig. 14 illustrates $|S_{11}|$ and $|S_{21}|$ compared between the simulated and measured results. The solid and dashed lines represent the simulated and measured results, respectively. The simulated and measured results are in reasonable agreement. At the center frequency, the simulated and measured $|S_{11}|$ are respectively -22.79 dB and -23.09 dB, whereas the simulated and measured $|S_{21}|$ are -46.54 dB and -33.99 dB, respectively. The impedance bandwidth ($|S_{11}| < -10$ dB) from the simulation is 15.16% (5.12–5.96 GHz), and that from the measurement is 23.64% (5.11–6.48 GHz). The obtained bandwidth can cover the requirement of WLAN system according to the IEEE802.11a standard. In addition, the isolation is relatively high. It thus can be concluded that the proposed antenna can be efficiently

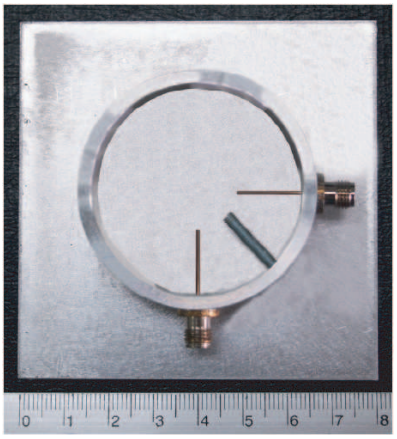

Figure 13. Photograph of the prototype antenna.

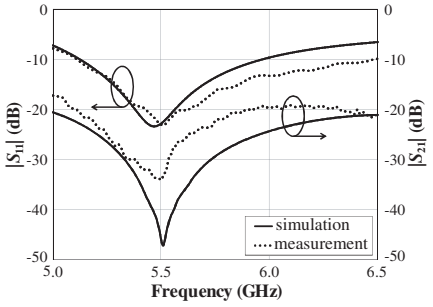

Figure 14. The comparison of $|S_{11}|$ and $|S_{21}|$ between simulation and measurement.

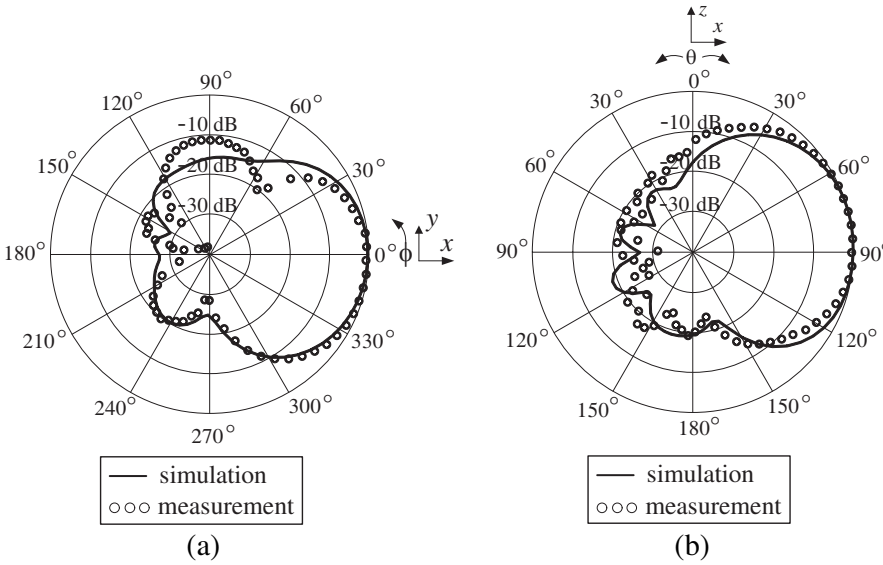

Figure 15. Simulated and measured radiation patterns with Probe1 excitation. (a) xy-plane. (b) xz-plane.

applied to polarization diversity reception.

The radiation patterns of the antenna were also measured. The measurement was carried out in two cases. The first case is performed for Probe1 excitation while Probe2 is terminated with a matched load. The measured results in xy-plane and xz-plane are superimposed with the simulated results as shown in Fig. 15. The second case is similar except that the antenna is excited at Probe2 while Probe1 is terminated with a matched load. The results are illustrated in Fig. 16. The solid and dashed lines represent the simulated and measured results, respectively. For both cases, the unidirectional pattern is achieved. From the symmetrical structure, the pattern with Probe1 excitation in xy-plane coincides with the excitation by Probe2 in xz-plane. The good agreement between the simulation and measurement is achieved. The simulated HPBW for Probe1 excitation in xy-plane and xz-plane are 60 and 80 degrees, respectively. For the measured results the HPBW are 65 and 75 degrees, respectively. The simulated and measured F/B are 26 dB and 31 dB, respectively. From the obtained results, it is apparent that this antenna possesses the good radiation pattern for polarization diversity of point-to-point communication.

The antenna gain was measured and compared with the simulated results as shown in Fig. 17. Both results display an identical trend with less than 2 dB difference. This discrepancy is due to the imperfect fabrication compared with the ideal simulation. For example, the loss

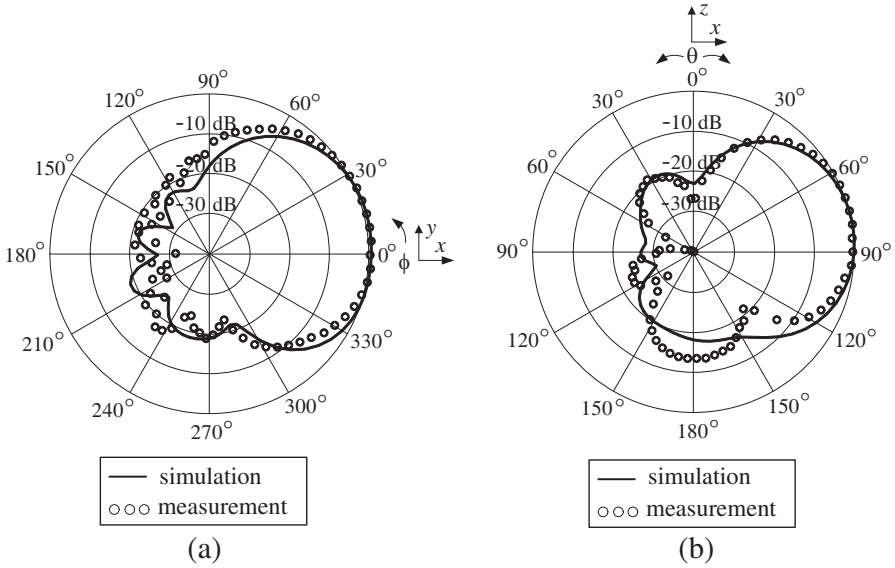

Figure 16. Simulated and measured radiation patterns with Probe2 excitation. (a) xy-plane. (b) xz-plane.

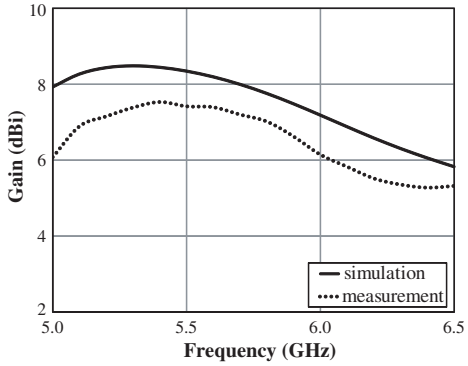

Figure 17. The simulated and measured gains.

tangent from the plastic rod that is used as the dielectic supporter between the circular ring and the square reflector was not taken into account in the simulation. It is obvious that the simulated (solid line) and measured (dashed line) gains at the center frequency are 8.35 dBi and 7.42 dBi, respectively. The variation of the gain along the bandwidth of 5.150–5.825 GHz is around 1 dB. This antenna thus has sufficient gain for point-to-point communication of WLAN system.

5. CONCLUSIONS

A unidirectional antenna for polarization diversity of WLAN system is achieved by using the circular ring excited by two perpendicular probes above the square reflector. The isolation is improved by adding a linear isolator at an angle of 45 degrees between two probes. The antenna principle is uncomplicated and the design straightforward. In addition, the prototype antenna is readily fabricated and conveniently produced on a mass scale. At the center frequency, the HPBW in two principal planes are 65 and 75 degrees, and the F/B is 31 dB. The obtained gain is 7.42 dBi. The antenna provides good radiation characteristics suitable for the point-to-point communication. $|S_{11}|$ and $|S_{21}|$ are -23.09 dB and -33.99 dB, respectively. The bandwidth can cover 5.11–6.48 GHz. It can be concluded that this antenna is appropriate for polarization diversity of WLAN system according to the IEEE802.11a standard. Furthermore, based on the antenna principle and design, the antenna parameters can be varied to realize the polarization diversity antenna of point-to-point communication in other wireless communication systems.

ACKNOWLEDGMENT

This work is financially supported by AUN/Seed-Net Program.

REFERENCES

1. IEEE Std. 802.11, Part 11, *Wireless LAN Medium Access Control (MAC) and Physical Layer (PHY) Specifications*, 1997.
2. IEEE Std. 802.11a, Supplement to Part 11, *Wireless LAN Medium Access Control (MAC) and Physical Layer (PHY) Specifications: Higher-Speed Physical Layer Extension in the 5 GHz Band*, 1999.
3. Chreim, H., E. Pointereau, B. Jecko, and P. Dufrane, "Omnidirectional electromagnetic band gap antenna for base station applications," *IEEE Antennas and Wireless Propagation Letters*, Vol. 6, 499–502, 2007.
4. Freytag, L., E. Pointereau, and B. Jecko, "Omnidirectional dielectric electromagnetic band gap antenna for base station of wireless network," *Proceedings of IEEE Antennas and Propagation Society International Symposium*, Vol. 1, 815–818, 2004.
5. Tsai, C.-L., "A coplanar-strip dipole antenna for broadband circular polarization operation," *Progress In Electromagnetics Research*, Vol. 121, 141–157, 2011.

6. Wounchoum, P., D. Worasawate, C. Phongcharoenpanich, and M. Krairiksh, "A switched-beam antenna using circumferential-slots on a concentric sectoral cylindrical cavity excited by coupling slots," *Progress In Electromagnetics Research*, Vol. 120, 127–141, 2011.
7. Eom, S.-Y., Y.-B. Jung, S. A. Ganin, and A. V. Shishlov, "A cylindrical shaped-reflector antenna with a linear feed array for shaping complex beam patterns," *Progress In Electromagnetics Research*, Vol. 119, 477-495, 2011.
8. Quan, X. L., R. L. Li, J. Y. Wang, and Y. H. Cui, "Development of a broadband horizontally polarized omnidirectional planar antenna and its array for base stations," *Progress In Electromagnetics Research*, Vol. 128, 441–456, 2012.
9. Wei, K. P., Z. J. Zhang, and Z. H. Feng, "Design of a dualband omnidirectional planar microstrip antenna array," *Progress In Electromagnetics Research*, Vol. 126, 101–120, 2012.
10. Li, R. L., T. Wu, and M. M. Tentzeris, "A triple-band unidirectional coplanar antenna for 2.4/3.5/5-GHz WLAN/WiMax applications," *Proceedings of IEEE Antennas and Propagation Society International Symposium*, 1–4, 2009.
11. Sze, J.-Y. and S.-P. Pan, "Design of broadband circularly polarized square slot antenna with a compact size," *Progress In Electromagnetics Research*, Vol. 120, 513–533, 2011.
12. Wang, X., M. Zhang, and S.-J. Wang, "Practicability analysis and application of PBG structures on cylindrical conformal microstrip antenna and array," *Progress In Electromagnetics Research*, Vol. 115, 495–507, 2011.
13. Fuschini, F., H. El-Sallabi, V. Degli-Esposti, L. Vuokko, D. Guiducci, and P. Vainikainen, "Analysis of multipath propagation in urban environment through multidimensional measurements and advanced ray tracing simulation," *IEEE Transactions on Antennas and Propagation*, Vol. 56, No. 3, 848–857, 2008.
14. Wang, X., Z. Du, and K. Gong, "A compact wideband planar diversity antenna covering UMTS and 2.4 GHz WLAN bands," *IEEE Antennas and Wireless Propagation Letters*, Vol. 7, 588–591, 2008.
15. Peng, H.-L., W.-Y. Yin, J.-F. Mao, D. Huo, X. Hang, and L. Zhou, "A compact dual-polarized broadband antenna with hybrid beam-forming capabilities," *Progress In Electromagnetics Research*, Vol. 118, 253–271, 2011.
16. Ding, Y., Z. Du, K. Gong, and Z. Feng, "A novel dual-

band printed diversity antenna for mobile terminals," *IEEE Transactions on Antennas and Propagation*, Vol. 55, No. 7, 2088–2096, 2007.

17. Toh, W., Z. Chen, X. Qing, and T. See, "A planar UWB diversity antenna," *IEEE Transactions on Antennas and Propagation*, Vol. 57, No. 11, 3467–3473, 2009.
18. Perini, P. L. and C. L. Holloway, "Angle and space diversity comparisons in different mobile radio environments," *IEEE Transactions on Antennas and Propagation*, Vol. 46, No. 6, 764–775, 1998.
19. Laneman, J. N., G. W. Wornell, and D. N. C. Tse, "An efficient protocol for realizing cooperative diversity in wireless networks," *Proceedings of IEEE Information Symposium on Information Theory*, 294, 2001.
20. Brown, T. W. C., R. Saunders, S. Stavrou, and M. Fiacco, "Characterization of polarization diversity at the mobile," *IEEE Transactions on Vehicular Technology*, Vol. 56, No. 5, 2440–2447, 2007.
21. Li, X., X. Huang, Z. Nie, and Y. Zhang, "Equivalent relations between interchannel coupling and antenna polarization coupling in polarization diversity systems," *IEEE Transactions on Antennas and Propagation*, Vol. 55, No. 6, 1709–1715, 2007.
22. Krairiksh, M., P. Keowsawat, C. Phongcharoenpanich, and S. Kosulvit, "Two-probe excited circular ring antenna for MIMO application," *Progress In Electromagnetics Research*, Vol. 97, 417–431, 2009.
23. Xie, J.-J., Y.-Z. Yin, J. Ren, and T. Wang, "A wideband dual-polarized patch antenna with electric probe and magnetic loop feeds," *Progress In Electromagnetics Research*, Vol. 132, 499–515, 2012.
24. Su, D., J. J. Qian, H. Yang, and D. Fu, "A novel broadband polarization diversity antenna using a cross-pair of folded dipoles," *IEEE Antennas and Wireless Propagation Letters*, Vol. 4, 433–435, 2005.
25. Eggers, P. C. F., J. Toftgard, and A. M. Oprea, "Antenna systems for base station diversity in urban small and micro cells," *IEEE Journal on Selected Areas in Communications*, Vol. 11, No. 7, 1046–1057, 1993.
26. Lee, B., S. Kwon, and J. Choi, "Polarization diversity microstrip base station antenna at 2 GHz using T-shaped aperture-coupled feeds," *Proceedings of IEE Microwave, Antennas and Propagation*, Vol. 148, No. 5, 334–338, 2001.

27. Dietrich, C. B., W. L. Stutzman, Jr., B. Kim, and K. Dietze, "Smart antennas in wireless communications: Base-station diversity and handset beamforming," *IEEE Antennas and Propagation Magazine*, Vol. 42, No. 5, 142–151, 2000.
28. Ou Yang, J., S. Bo, J. Zhang, and Y. Feng, "A low-profile unidirectional cavity-backed log-periodic slot antenna," *Progress In Electromagnetics Research*, Vol. 119, 423–433, 2011.
29. Xie, J.-J., Y.-Z. Yin, C. W. Zhang, and B. Li, "A novel trapezoidal slot patch antenna with a beveled ground plane for WLAN/WIMAX applications," *Progress In Electromagnetics Research Letters*, Vol. 27, 53–62, 2011.
30. Cai, D. S., Z.-Y. Lei, H. Chen, G.-L. Ning, and R. B. Wang, "Crossed oval-ring slot antenna with triple-band operation for WLAN/WIMAX applications," *Progress In Electromagnetics Research Letters*, Vol. 27, 141–150, 2011.
31. Liu, W.-C. and Y. Dai, "Dual-broadband twin-pair inverted-L shaped strip antenna for WLAN/WIMAX applications," *Progress In Electromagnetics Research Letters*, Vol. 27, 63–73, 2011.
32. Wang, X.-M., Z.-B. Weng, Y.-C. Jiao, Z. Zhang, and F.-S. Zhang, "Dual-polarized dielectric resonator antenna with high isolation using hybrid feeding mechanism for WLAN applications," *Progress In Electromagnetics Research Letters*, Vol. 18, 195–203, 2010.
33. Rezaeieh, S. A. and M. Kartal, "A new triple band circularly polarized square slot antenna design with crooked T and F-shape strips for wireless applications," *Progress In Electromagnetics Research*, Vol. 121, 1–18, 2011.
34. Panda, J. R. and R. S. Kshetrimayum, "A printed 2.4 GHz/5.8 GHz dual-band monopole antenna with a protruding stub in the ground plane for WLAN and RFID applications," *Progress In Electromagnetics Research*, Vol. 117, 425–434, 2011.
35. Weng, W.-C. and C.-L. Hung, "Design and optimization of a logo-type antenna for multiband applications," *Progress In Electromagnetics Research*, Vol. 123, 159–174, 2012.
36. CST-Microwave Studio, User's Manual, 2006.
37. Kosulvit, S., M. Krairiksh, C. Phongcharoenpanich, and T. Wakabayashi, "A simple and cost-effective bidirectional antenna using a probe excited circular ring," *IEICE Trans. Electronics*, Vol. E84-C, No. 4, 443–450, 2001.